P69 COMPARISON OF FOUR PRECIPITATION FORCING DATASETS IN LAND INFORMATION SYSTEM SIMULATIONS OVER THE CONTINENTAL U.S.

Jonathan L. Case*[1], Sujay V. Kumar[2], Robert J. Kuligowski[3], and Carrie Langston[4]

[1]*ENSCO, Inc./Short-term Prediction Research and Transition (SPoRT) Center, Huntsville, AL*
[2]*SAIC/NASA Goddard Space Flight Center, Greenbelt, MD;*
[3]*NOAA/NESDIS/Center for Satellite Applications and Research, Camp Springs, MD;*
[4]*Cooperative Institute for Mesoscale Meteorological Studies (CIMMS), Norman, OK*

1. INTRODUCTION

The NASA Short-term Prediction Research and Transition (SPoRT) Center in Huntsville, AL is running a real-time configuration of the Noah land surface model (LSM) within the NASA Land Information System (LIS) framework (hereafter referred to as the "SPoRT-LIS"). Output from the real-time SPoRT-LIS is used to initialize land surface variables for local modeling applications, and is displayed in decision support systems for situational awareness and drought monitoring at select National Weather Service (NWS) partner offices. The SPoRT-LIS is run over a domain covering the southeastern portion of the Continental United States (CONUS), fully nested within the National Centers for Environmental Prediction (NCEP) Stage IV precipitation analysis grid, which provides precipitation forcing to the offline LIS-Noah runs.

The SPoRT Center seeks to expand the real-time LIS domain to the entire CONUS; however, geographical boundaries and other limitations with the Stage IV analysis product have inhibited this expansion. Therefore, a goal of this study is to test alternative precipitation forcing datasets with coverage encompassing the entire CONUS region that can enable a SPoRT-LIS expansion to a full CONUS domain.

For this paper, four hourly precipitation datasets used to force experimental LIS integrations for one year are inter-compared on a CONUS domain with 3-km grid spacing:

- North American Land Data Assimilation System phase 2 (NLDAS2) hourly analyses,
- NCEP Stage IV hourly precipitation,
- Next generation Geostationary Operational Environmental Satellite (GOES) quantitative precipitation estimate (QPE) algorithm from NESDIS/STAR, and
- National Mosaic and QPE (NMQ) product from the National Severe Storms Laboratory (NSSL).

The ultimate goal is to identify an alternative precipitation forcing dataset that can best support an expansion of the real-time SPoRT-LIS to a domain covering the entire CONUS.

**Corresponding author address:* Jonathan Case, ENSCO, Inc., 320 Sparkman Dr., Room 3008, Huntsville, AL, 35805. Email: Jonathan.Case-1@nasa.gov

Section 2 gives background information on the NASA LIS and the current real-time SPoRT-LIS configuration. Section 3 describes the precipitation datasets and configuration / methodology used for the LIS simulation experiments. Preliminary results are shown in Section 4 followed by a summary and future work in Section 5.

2. NASA LAND INFORMATION SYSTEM AND SPORT-LIS CONFIGURATION

2.1 LIS software framework

The NASA LIS is a high performance land surface modeling and data assimilation system that integrates satellite-derived datasets, ground-based observations and model reanalyses to force a variety of LSMs (Kumar et al. 2006; Peters Lidard et al. 2007). By using scalable, high-performance computing and data management technologies, LIS can run LSMs offline globally with a grid spacing as fine as 1 km to characterize land surface states and fluxes. LIS has also been coupled to the Advanced Research Weather Research and Forecasting dynamical core (Kumar et al. 2007) for numerical weather prediction (NWP) applications.

2.2 SPoRT-LIS Description

In the SPoRT-LIS, version 3.2 of the Noah LSM (Ek et al. 2003; Chen and Dudhia 2001) is run offline (i.e. uncoupled from an NWP model) over a southeastern CONUS domain at 3-km grid spacing for a continuous long simulation. The soil temperature and volumetric soil moisture fields are initialized at constant values of 290 K and 20% in all four Noah soil layers (0-10, 10-40, 40-100, and 100-200 cm).

2.2.1 **Static input fields**

The SPoRT-LIS uses the International Geosphere-Biosphere Programme (IGBP) land-use classification (Loveland et al. 2000) as applied to the Moderate Resolution Imaging Spectroradiometer (MODIS) instrument (Friedl et al. 2010). All static and dynamic land surface fields are masked based on the IGBP/MODIS land-use classes. The soil properties are represented by the State Soil Geographic (STATSGO; Miller and White 1998) database.

Additional required parameters include a 0.05° resolution maximum snow surface albedo derived

from MODIS (Barlage et al. 2005) and a deep soil temperature climatology (serving as a lower boundary condition for the soil layers) at 3 meters below ground, derived from 6 years of Global Data Assimilation System (GDAS) 3-hourly averaged 2-m air temperatures using the method described in Chen and Dudhia (2001). In addition, real-time green vegetation fraction (GVF) data derived from MODIS normalized difference vegetation index (NDVI) data (Case et al. 2011) are incorporated into the LIS runs in place of the default monthly climatology GVF dataset (Gutman and Ignatov 1998). The real-time MODIS GVF are produced by SPoRT on a CONUS domain with 0.01° (~1 km) grid spacing, and updated daily with new MODIS NDVI swath data.

2.2.2 **Simulation and atmospheric forcing**

The Noah LSM simulation in the recently-upgraded SPoRT-LIS configuration (Case et al. 2012) was initialized at 0000 UTC 1 June 2010, coinciding with the first day of availability of the real-time SPoRT-MODIS GVF. The simulation was run for over two years prior to use for real-time applications (effective September 2012), in order to ensure that no memory of the unrealistic uniform soil initial conditions was retained. The atmospheric forcing variables required to drive the LIS/Noah integration consist of surface pressure, 2-m temperature and specific humidity, 10-m winds, downward-directed shortwave and longwave radiation, and precipitation rate. In the long-term simulation, all atmospheric forcing variables are provided by hourly analyses from the North American Land Data Assimilation System phase 2 (NLDAS2; Xia et al. 2012), except for precipitation, where hourly precipitation analyses from the NCEP Stage IV precipitation product (Lin and Mitchell 2005; Lin et al. 2005) are used. The grid spacing of the NLDAS2 analyses is one-eighth degree (~14 km) whereas the Stage IV analyses have ~4.8 km grid spacing. The Noah LSM solution ultimately converges to a modeled state based on the NLDAS2 and Stage IV precipitation input.

The Stage IV precipitation analyses are typically available within an hour or two of the current time. However, limitations associated with the temporal availability of NLDAS2 analyses in real time warrant the use of alternative datasets in order to provide timely SPoRT-LIS output to end users each day. Currently, the NLDAS2 forcing files are only available through about four days prior to the current day. Therefore, to integrate LIS/Noah from the time availability of NLDAS2 to approximately the current time, the LIS is re-started using atmospheric forcing files from the NCEP GDAS (Parrish and Derber 1992; NCEP EMC 2004), along with a continuation of the Stage IV hourly precipitation. The GDAS contains 0–9 hour short-range forecasts of the required atmospheric forcing variables at 3-hourly intervals, derived from the data assimilation cycle of the NCEP Global Forecast System (GFS) model. The GDAS files are available about 6–7 hours after the valid GFS forecast cycle (e.g. GDAS 0–9 h files from the 1200 UTC forecast cycle are available approximately between 1800 UTC and 1900 UTC).

Finally, to ensure continuous availability of SPoRT-LIS output for initializing LSM fields in local modeling applications, an additional LIS re-start is made driven by atmospheric forcing from the NCEP GFS model 3–15 hour forecasts. The small predictive component of the SPoRT-LIS is done in order to capture the diurnal heating cycle impact on surface energy fluxes. The short-range SPoRT-LIS output then is provided to the NWS Birmingham, AL forecast office in support of their convective initiation and summer precipitation prediction activities, which includes real-time SPoRT-LIS output in their forecast process (Goggins et al. 2010; Unger et al. 2011).

The SPoRT-LIS cycle is initiated four times daily at 0400, 1000, 1600, and 2200 UTC with the history re-starts of the LIS simulation as described above. In each cycle, the first re-start simulation begins 5 days before the current time, over-writing previous output files to ensure a model convergence towards NLDAS2 + Stage IV precipitation forcing. For further clarity, the structure and timing of the real-time LIS simulation and history re-starts are illustrated in Figure 1.

3. PRECIPITATION DATASETS AND EXPERIMENT METHODOLOGY

The NLDAS2 dataset is used as the control run, with each of the other three datasets considered experimental runs compared to the control. The characteristics of each precipitation dataset are described below. The regional strengths, weaknesses, and biases of each precipitation analysis are identified relative to the NLDAS2 control in terms of accumulated precipitation pattern and amount, and the impacts on the subsequent LIS-Noah LSM spin-up simulations.

3.1 NLDAS2

The precipitation fields in the NLDAS2 product consist of hourly accumulated precipitation on a 0.125° grid with coverage over northern Mexico, the CONUS, and southern Canada (i.e. from 25° to 52° N latitude). Precipitation fields are blended from a combination of data from the 3-hour North American Regional Reanalysis (NARR), daily Climate Prediction Center (CPC) rain gauges, 0.5-hour CPC Morphing (CMORPH) technique fields, hourly NCEP Stage II data, and the PRISM topographical adjustment (Daly et al. 1994). The daily CPC gauges are temporally disaggregated into hourly totals based on Stage II radar information.

3.2 Stage IV

The NCEP Stage IV precipitation analyses are generated in near real time on a 4.8-km grid over much of the CONUS. The hourly accumulated precipitation fields are a combination of radar rain rates and gauge observations. The Stage IV analyses receive contributions from the various River Forecast Centers across the U.S., so some real-time products do not contain contributions in certain regions. One limitation to the Stage IV grid is its odd-shaped polygon grid, which cuts off portions of the Pacific NW, southern Canada, and northern Mexico (Figure 2). As a result, sharp artificial gradients in simulated soil moisture result when Stage IV data are used in a CONUS LIS integration.

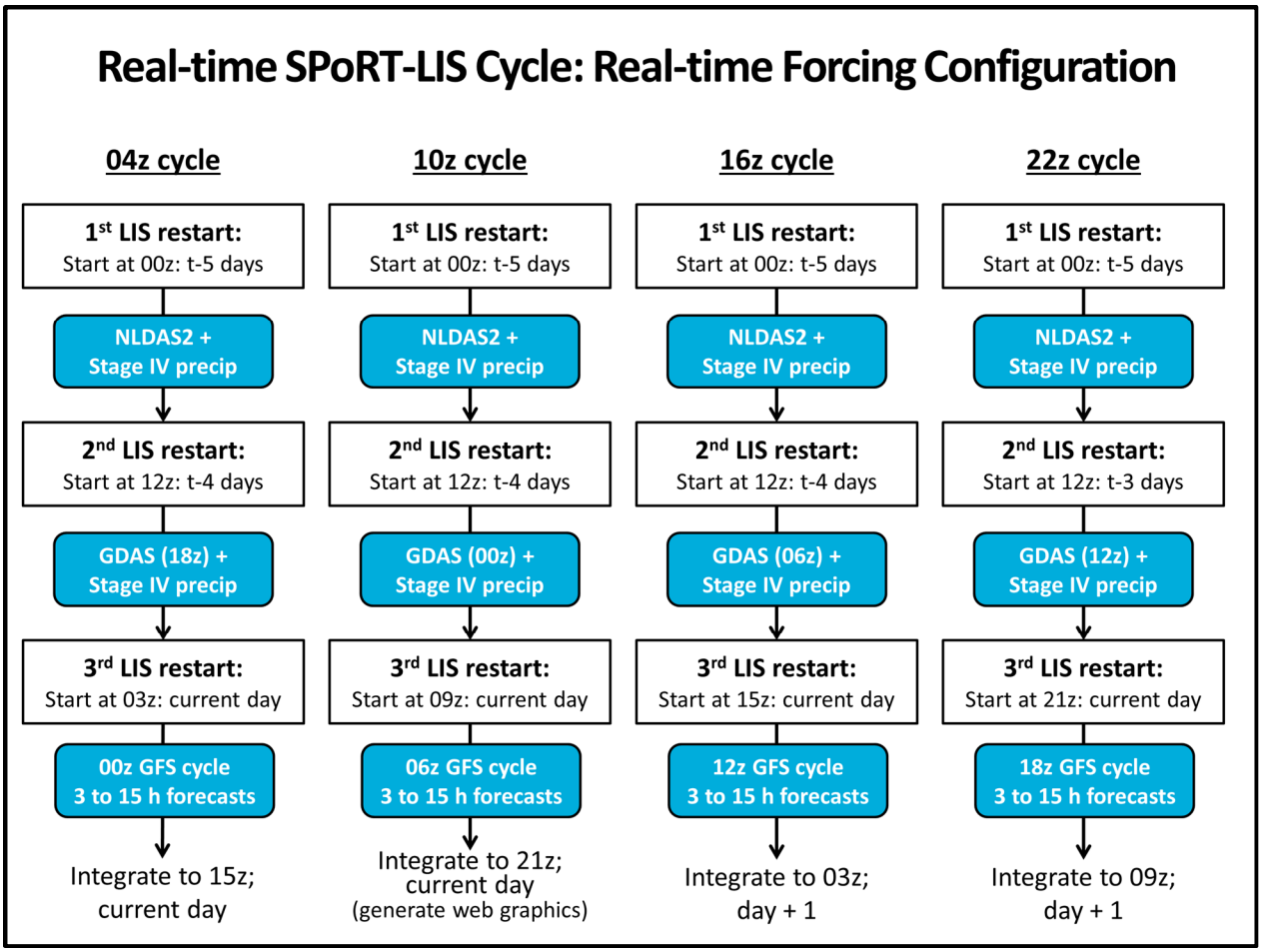

Figure 1. Diagram outlining the structure and timing of the real-time SPoRT-LIS simulation, conducted four times daily at 0400, 1000, 1600, and 2200 UTC. Each history re-start simulation is a continuation of the single long integration that was initialized at 0000 UTC 1 June 2010. Output is over-written by each new re-start to ensure the simulation converges to a modeled state based on NLDAS2 and Stage IV precipitation forcing.

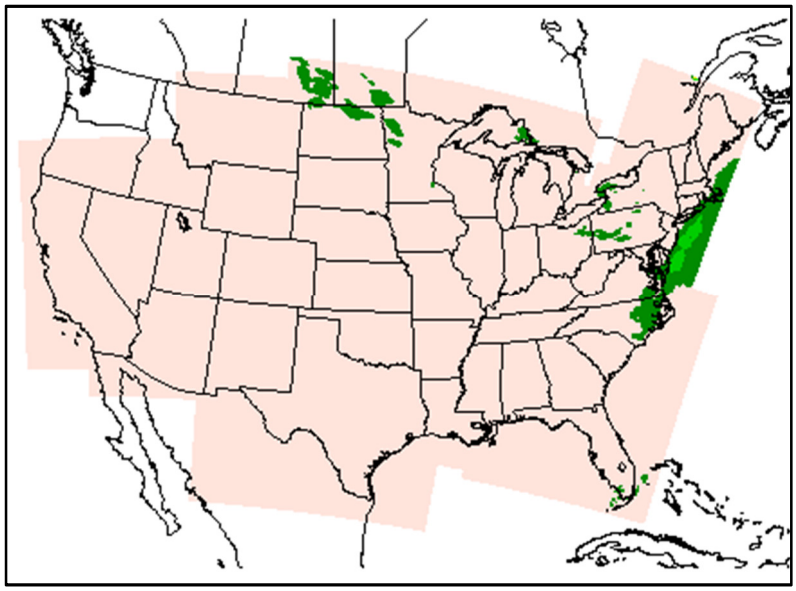

Figure 2. Geographical extent of the NCEP Stage IV analysis domain, given by the polygon shaded region.

3.3 National Mosaic QPE (NMQ)

The NSSL NMQ (Zhang et al. 2011) is a high-resolution, hourly precipitation product (with optional finer time scales) analyzed on a 0.01° grid (~1 km) extending from northern Mexico to southern Canada. It is a similar blended radar / rain gauge product as the Stage IV, but with greater geographical coverage and nearly 5 times the grid resolution. The primary limitation experienced with the database tested for this experiment is that it has zero values assigned in data-void regions instead of assigning missing values. Also, radar coverage gaps show up quite distinctly in the intermountain U.S. West, especially in the winter months when precipitation systems tend to be shallower with less detection ability of the radars.

3.4 NESDIS/STAR next generation GOES QPE

This experimental precipitation product (based on Kuligowski 2002) is developed using current-generation GOES IR data calibrated against microwave satellite measurements to estimate precipitation on a ~4-km grid. It is the official GOES-R algorithm working group product for the next generation in geostationary satellites forthcoming. The coverage of the GOES next generation QPE is the most extensive of any of the precipitation products, with coverage over much of the western hemisphere. However, like any purely satellite-based precipitation algorithm, it has challenges with QPE in stratiform regions and areas with an extensive high cirrus canopy. In these situations, precipitation tends to be over-estimated compared to radar/gauge-based techniques.

3.5 LIS integration methodology

The LIS integration for the precipitation forcing comparison follows a similar configuration to that of the current real-time SPoRT-LIS, except for using an expanded CONUS domain with the same 3-km grid spacing. A one-year simulation is conducted from 1 September 2011 to 1 September 2012 using the same initialization as described in the previous section for the SPoRT-LIS. All the same static parameters as in the SPoRT-LIS are used in these experimental one-year simulations. Atmospheric forcing in the control LIS run is provided by hourly NLDAS2 analyses with background forcing fields given by 3-hourly GDAS files outside of the geographical coverage of NLDAS2 (i.e. small parts of the CONUS LIS domain in southern Canada and northern Mexico). The experimental LIS runs have the same configuration as the control, except that NLDAS2 precipitation is replaced by Stage IV, NMQ, and GOES QPE, respectively.

4. PRELIMINARY RESULTS OF LIS SIMULATIONS

The LIS integrations were made not only to assess the impact of the precipitation datasets on the Noah soil moisture fields, but also to examine the accumulated precipitation fields in 30-day intervals throughout the year. Comparisons of 30-day accumulated precipitation fields show the varying level of details and help reveal biases of each dataset relative to one another.

4.1 Thirty-day accumulated precipitation fields

Figure 3 presents a summary of 30-day accumulated precipitation fields at quarterly intervals from October 2011 to July 2012. The control precipitation (NLDAS2) is shown in the left-most column and compared to Stage IV (2nd column from left), NMQ (3rd column) and GOES QPE (4th column). A general observation is that the radar/gauge-based datasets (NLDAS2, Stage IV, and NMQ) exhibit the most similar patterns to one another in each 30-day period, especially east of the Rockies. The GOES QPE satellite-based estimates in column 4 are consistently higher in both spatial coverage and intensity compared to the other three datasets.

We now examine more of the details in each dataset, beginning with Stage IV in column 2. The first consistent issue noted with the Stage IV accumulated precipitation is the anomalously low precipitation amounts in a couple "patches" across southeastern Canada. In each quarter, low values are seen near the northeast edges of the Stage IV grid (Figure 2) leading to sharp artificial gradients in 30-day accumulated precipitation. This problem is likely due to these patches being outside of radar and/or gauge coverage. In January 2012, the artificial minimum extends from the westernmost patch across southern Canada along the northern edge of the Stage IV grid boundary. Additional problems with the Stage IV accumulated precipitation occur in the western U.S. from southern Oregon south to the Mexico border. It appears that data are consistently missing in California and Nevada throughout the year. It may be necessary to acquire the archived hourly Stage IV precipitation files for the integration period to determine if the real-time acquisition consistently results in incomplete files.

The NMQ (column 3) shows similar patterns to the Stage IV (particularly east of the Rockies) but with a little more detail due to its higher resolution grid (~1 km spacing vs. ~4.8 km spacing in Stage IV). The influence of radar range rings in the precipitation analysis is more pronounced in the NMQ analyses, especially in the western U.S. and southern Canada where radar and gauge coverage tends to be less than in other regions. In addition, gaps in radar coverage in the intermountain West result in near zero precipitation amounts that correlate closely to these gaps (not shown), especially in the cool-season months when the depth of precipitation systems tends to be shallower and thus over-shot by the radar beams in the complex terrain. In addition, with the NMQ domain extending further north and south of the images shown, values are set to zero (instead of missing) in areas where no input data exist in Canada and Mexico. This is a characteristic of the NMQ dataset used for this experiment and could be amended in the future.

As noted earlier, the GOES QPE has far too much precipitation in the analysis over too great an area. Future versions of the GOES QPE algorithm should address this consistent over-representation of precipitation. For now, it appears that the GOES-R precipitation algorithm is not yet suitable for use in land surface modeling applications.

4.2 Impacts on soil moisture distribution

The root zone relative soil moisture distribution (40-100 cm layer of LIS-Noah; Figure 4) generally follow the precipitation patterns closely. The NLDAS2 experiment (serving as the control run) generally has the smoothest and most realistic looking gradients in soil moisture distribution, except in July 2012 when an artificial high precipitation bulls-eye occurs in southern Ontario between Lakes Huron and Ontario (bottom-left panel of Figure 3 and Figure 4; likely caused by input precipitation data from the NARR that is not being blended correctly). The extent of the summer 2012 drought is quite apparent in the soil moisture minimum that covers much of the Midwest and Plains (relative soil moisture < 5% in bottom panel of column 1 in Figure 4).

The broad soil moisture patterns in the Stage IV run (column 2 of Figure 4) closely follow the NLDAS2 run, except in the problem areas noted in the previous sub-section. Artificial soil moisture gradients can be seen in southeastern Canada and the Pacific Northwest states, with artificially low values in California and Nevada due to the low accumulated precipitation anomaly as described earlier. Problems can also be seen in parts of Mexico in July 2012.

The NMQ run (column 3 of Figure 4) also exhibits similar soil moisture patterns to the NLDAS2 run in each month, except that the radar cut-off patterns are more pronounced in southern Canada. Soil moisture is too dry in Mexico and parts of Canada relative to NLDAS2, particularly by July 2012.

The GOES QPE run (column 4) has the most disparate root-zone soil moisture patterns compared to the NLDAS2 control run due to the exceedingly high coverage and intensity of precipitation. The most severe biases in soil moisture compared to NLDAS2 are seen in April 2012 over the northwest quarter of the CONUS. Severe wet biases are also seen in much of the eastern CONUS, Upper Midwest, and High Plains during July 2012. The drought is somewhat captured in the Plains, given by a fairly large area of relatively drier soil moisture. However, almost the entire domain suffers from an overall wet bias due to over-estimated precipitation.

4.3 Experiment with NMQ to improve areas with radar gaps and zero values

An experimental run was made to help alleviate the radar gap issues in the NMQ precipitation analyses over the intermountain West of the CONUS, Mexico, and parts of southern Canada. In this simple experiment, NMQ precipitation superseded the NLDAS2 only when NMQ values were non-zero. The idea is that consist problem areas where NMQ has no available data and thus grid point values of zero are not used, thereby retaining the background NLDAS2 precipitation values. The same concept could be used with the Stage IV dataset in its problem areas over southeastern Canada, Mexico, and the western CONUS. However, we would first like to download archived Stage IV precipitation analyses to determine whether this improves the problems in California and Nevada.

The results of this "NMQ > 0" experiment are presented in column 4 of Figure 5 and Figure 6 (in place of the GOES QPE results) while retaining the original NLDAS2, Stage IV, and NMQ experiment results in columns 1 through 3, respectively, for comparison purposes. In each quarter, the 30-day accumulated precipitation fields are wetter overall in the NMQ > 0 run compared to the original NMQ LIS run. However, the radar gap problems out West appear to be significantly improved in the NMQ > 0 simulation, particularly from October 2011 to April 2012 (column 4 of Figure 5). The zero precipitation areas in Mexico and Canada have assumed the background NLDAS2 values, as expected. The net result is a much more appealing distribution of precipitation in each month presented, with generally smooth and realistic-looking gradients and transition zones. Many of the high-resolution details of the original NMQ simulation are still retained.

An examination of the precipitation and soil moisture difference fields from July 2012 in Figure 7 reveals the impacts of the NMQ > 0 experiment. First, the NMQ – NLDAS2 differences in the first column show that NMQ was consistently higher in July 2012 over the U.S. High Plains and southern Canada, indicative of the contributions from radar data at higher resolution. The radar gaps in the intermountain West show up as negative precipitation differences, whereas the problem with zero values over Canada and Mexico have the most negative precipitation differences, and subsequently negative soil moisture differences.

When only non-zero NMQ precipitation replaces the NLDAS2 precipitation (column 2), the negative differences disappear in Canada and Mexico since NLDAS2 values prevail there. [The negative bulls-eye in southern Ontario, Canada is indicative of the problem with the NLDAS2 precipitation alluded to earlier.] Many of the negative precipitation differences in the intermountain West from NMQ – NLDAS2 disappear in the NMQ > 0 – NLDAS2 difference plot. In general, positive precipitation differences remain over much of the domain in areas where NMQ data exist, leading to higher root zone soil moisture in many areas (bottom of column 2). A strong influence of radar contribution and beam blockage is evident in the soil moisture difference field in the intermountain West.

Finally, the difference fields between the NMQ > 0 and NMQ simulations (3rd column) show how the resulting 30-day precipitation only increases in much of the domain (top-right panel). The resulting root zone soil moisture difference shows that more moist conditions prevail most everywhere, except in the Midwest region plagued by drought in July 2012 (bottom-right panel of Figure 7). Much of the soil moistening that occurs is a result of the accumulation of 11 months of precipitation differences between the NMQ > 0 and NMQ simulations. Besides Canada and Mexico, the most substantial soil moistening in NMQ > 0 occurs in the southeastern U.S. and Pacific Northwest.

5. SUMMARY AND FUTURE WORK

This paper and poster presented a description of the current real-time SPoRT-LIS run over the southeastern CONUS to provide high-resolution, land surface initialization grids for local numerical model forecasts at NWS forecast offices. The LIS hourly output also offers a supplemental dataset to aid in situational awareness for convective initiation forecasts, assessing flood potential, and monitoring drought at fine scales.

It is a goal of SPoRT and several NWS forecast offices to expand the LIS to an entire CONUS domain, so that LIS output can be utilized by NWS Western Region offices, among others. To make this expansion cleanly so as to provide high-quality land surface output, SPoRT tested new precipitation datasets in LIS as an alternative forcing dataset to the current radar+gauge Stage IV product. Similar to the Stage IV product, the NMQ product showed comparable patterns of precipitation and soil moisture distribution, but suffered from radar gaps in the intermountain West, and incorrectly set values to zero instead of missing in the data-void regions of Mexico and Canada.

The other dataset tested was the next-generation GOES-R QPE algorithm, which experienced a high bias in both coverage and intensity of accumulated precipitation relative to the control (NLDAS2), Stage IV, and NMQ simulations. The resulting root zone soil moisture was substantially higher in most areas.

Future efforts towards an expanded real-time LIS domain include the examination of yet more alternative precipitation datasets such as the TRMM microwave product (3B42RT) and the precipitation product generated by Environment Canada. A more quantitative evaluation of the LIS-Noah output is warranted through comparisons to in situ soil measurements such as those in the Soil Climate Analysis Network (Schaefer et al. 2007). Additionally, SPoRT plans to assimilate soil moisture retrievals using the Ensemble Kalman filter algorithm within LIS (Kumar et al. 2008; Kumar et al. 2009). Assimilating soil moisture retrievals should help improve the modeled soil moisture fields, especially in areas where the precipitation forcing datasets do not have good data coverage or representativeness.

ACKNOWLEDGEMENTS/DISCLAIMER

This research was funded by Dr. Tsengdar Lee of the NASA Science Mission Directorate's Earth Science Division in support of the SPoRT program at the NASA MSFC. Mention of a copyrighted, trademarked or proprietary product, service, or document does not constitute endorsement thereof by the authors, ENSCO Inc., SAIC, CIMMS, the SPoRT Center, the National Aeronautics and Space Administration, the National Oceanic and Atmospheric Administration, or the United States Government. Any such mention is solely for the purpose of fully informing the reader of the resources used to conduct the work reported herein.

REFERENCES

Barlage, M., X. Zeng, H. Wei, and K. E. Mitchell, 2005: A global 0.05° maximum albedo dataset of snow-covered land based on MODIS observations. *Geophys. Res. Lett.,* **32,** L17405, doi:10.1029/2005GL022881.

Case, J. L., F. J. LaFontaine, S. V. Kumar, and G. J. Jedlovec, 2011: A real-time MODIS vegetation composite for land surface models and short-term forecasting. Preprints, *15th Symp. on Integrated Observing and Assimilation Systems for the Atmosphere, Oceans, and Land Surface,* Seattle, WA, Amer. Meteor. Soc., 11.2. [Available online at http://ams.confex.com/ams/91Annual/webprogram/Manuscript/Paper180639/Case_etal_2011AMS-15IOAS-AOLS_11.2_FINAL.pdf]

Case, J. L., F. J. LaFontaine, A. L. Molthan, B. T. Zavodsky, and R. A. Rozumalski, 2012: Recent upgrades to NASA SPoRT initialization datasets for the Environmental Modeling System. Preprints, *37th National Weather Association Annual Meeting,* Madison, WI, National Weather Association, P1.40. [Available online at www.nwas.org/meetings/nwa2012/extendedabstracts/NWA2012_P1.40_Case_etal.pdf]

Chen, F., and J. Dudhia, 2001: Coupling an advanced land-surface/hydrology model with the Penn State/NCAR MM5 modeling system. Part I: Model description and implementation. *Mon. Wea. Rev.,* **129,** 569-585.

Daly, C., R. P. Neilson, and D. L. Phillips, 1994: A statistical-topographic model for mapping climatological precipitation over mountainous terrain. *J. Appl. Meteor.,* **33,** 140-158.

Ek, M. B., K. E. Mitchell, Y. Lin, E. Rogers, P. Grunmann, V. Koren, G. Gayno, and J. D. Tarpley, 2003: Implementation of Noah land surface model advances in the National Centers for Environmental Prediction operational mesoscale Eta model. *J. Geophys. Res.,* **108 (D22),** 8851, doi:10.1029/2002JD003296.

Friedl, M. A., D. Sulla-Menashe, B. Tan, A. Schneider, N. Ramankutty, A. Sibley, and X. Huang, 2010: MODIS Collection 5 global land cover: Algorithm refinements and characterization of new datasets. *Remote Sens. Environ.,* **114,** 168-182.

Goggins, G. D., M. L. Grantham, S. W. Unger, K. B. Laws, K. L. Pence, and L. Dawson, 2010: Analysis of summer convection over central Alabama. Preprints, *15th Symp. on Meteorological Observation and Instrumentation.* Atlanta, GA, Amer. Meteor. Soc, 9.2. [Available online at http://ams.confex.com/ams/pdfpapers/161408.pdf]

Gutman, G. and A. Ignatov, 1998: Derivation of green vegetation fraction from NOAA/AVHRR for use in numerical weather prediction models. *Int. J. Remote Sensing,* **19,** 1533-1543.

Kuligowski, R. J., 2002: A self-calibrating real-time GOES rainfall algorithm for short-term rainfall estimates. *J. Hydrometeor.,* **3,** 112-130.

Kumar, S. V., and Coauthors, 2006. Land Information System – An Interoperable Framework for High Resolution Land Surface Modeling. *Environmental Modeling & Software,* **21 (10),** 1402-1415, doi:10.1016/j.envsoft.2005.07.004.

Kumar, S. V., C. D. Peters-Lidard, J. L. Eastman, and W.-K. Tao, 2007: An integrated high-resolution hydrometeorological modeling testbed using LIS and WRF. *Environmental Modeling & Software,* **23 (2),** 169-181, doi: 10.1016/j.envsoft.2007.05.012.

Kumar, S. V., R. H. Reichle, R. D. Koster, W. T. Crow, and C. D. Peters-Lidard, 2009: Role of subsurface physics in the assimilation of surface soil moisture observations. *J. Hydrometeor.,***10,** 1534-1547.

Kumar, S. V., R. H. Reichle, C. D. Peters-Lidard, R. D. Koster, X. Zhan, W. T. Crow, J. B. Eylander, and P. R. Houser, 2008: A land surface data assimilation framework using the land information system: Description and applications. *Adv. Water Res.,***31,** 1419-1432.

Loveland, T. R., B. C. Reed, J. F. Brown, D. O. Ohlen, Z. Zhu, L. Yang, and J. W. Merchant, 2000: Development of a global land cover characteristics database and IGBP DISCover from 1 km AVHRR data. *Int. J. Remote Sensing,* **21,** 1303-1330.

Miller, D. A. and R. A. White, 1998: A Conterminous United States multi-layer soil characteristics data set for regional climate and hydrology modeling. *Earth Interactions*, 2. [Available on-line at http://EarthInteractions.org].

Lin, Y., and K. E. Mitchell, 2005: The NCEP Stage II/IV hourly precipitation analyses: Development and applications. Preprints, *19th Conf. on Hydrology,* San Diego, CA, Amer. Meteor. Soc., 1.2. [Available online at http://ams.confex.com/ams/pdfpapers/83847.pdf]

Lin, Y., K. E. Mitchell, E. Rogers, and G. J. DiMego, 2005: Using hourly and daily precipitation analyses to improve model water budget. Preprints, *Ninth Symp. on Integrated Observing and Assimilation Systems for the Atmosphere, Oceans, and Land Surface*, San Diego, CA, Amer. Meteor. Soc., 3.3. [Available online at http://ams.confex.com/ams/pdfpapers/84484.pdf]

NCEP Environmental Modeling Center, 2004: SSI Analysis System 2004. NOAA/NCEP/Environmental Modeling Center Office Note 443, 11 pp., April, 2004. [Available online at http://www.emc.ncep.noaa.gov/officenotes/newernotes/on443.pdf]

Parrish, D. F., and J. C. Derber, 1992: The National Meteorological Center's spectral statistical-interpolation analysis system. *Mon. Wea. Rev.,* **120,** 1747-1763.

Peters-Lidard, C. D., and Coauthors, 2007: High-performance Earth system modeling with NASA/GSFC's Land Information System. *Innovations Syst. Softw. Eng.,* **3,** 157-165.

Schaefer, G. L., M. H. Cosh, and T. J. Jackson, 2007: The USDA Natural Resources Conservation Service Soil Climate Analysis Network (SCAN). *J. Atmos. Oceanic Technol.,* **24,** 2073-2077.

Unger, S. W., K. B. Laws, G. D. Goggins, J. Talley, T. N. Golden, H. M. Britton, and J. Case, 2011: Overview of summer convection study over central Alabama. Abstracts, *36th Annual National Weather Association Meeting,* Birmingham, AL, National Weather Association, 76.

Xia, Y., and Coauthors, 2012: Continental-scale water and energy flux analysis and validation for the North American Land Data Assimilation System project phase 2 (NLDAS-2): 1. Intercomparison and application of model products. *J. Geophys. Res.*, **117,** 27 pp. doi:10.1029/2011JD016048.

Zhang J., and Coauthors, 2011: National Mosaic and multi-sensor QPE (NMQ) system: Description, results, and future plans. *Bull. Amer. Meteor. Soc.,* **92,** 1321-1338.

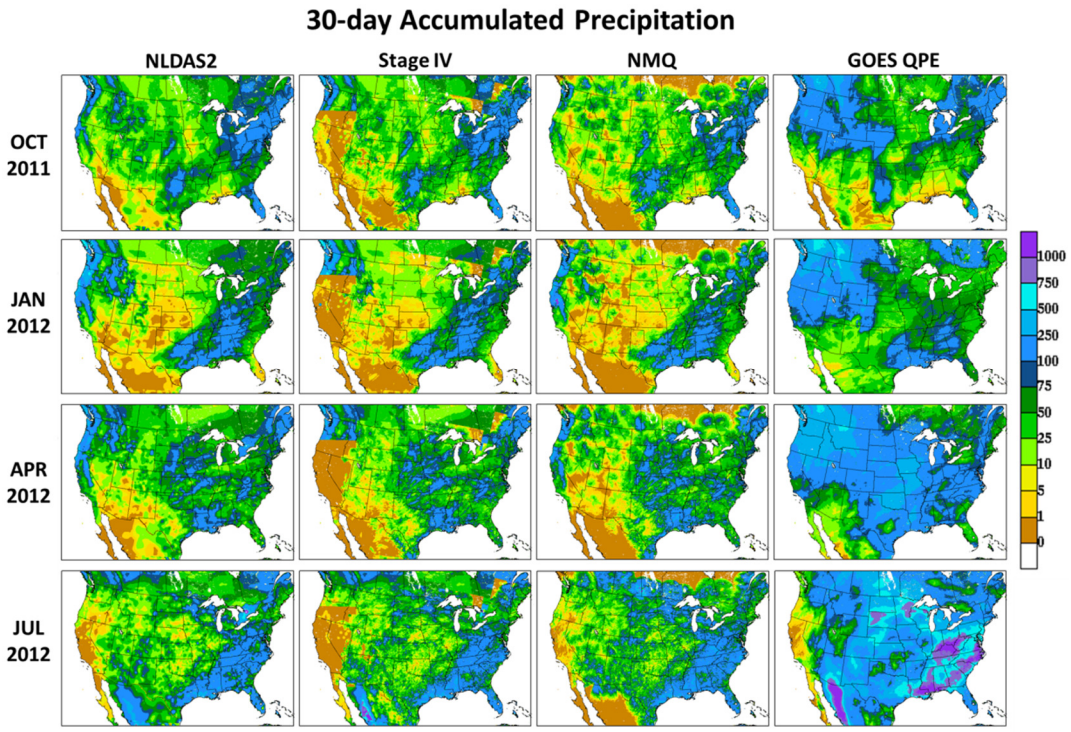

Figure 3. Thirty-day accumulated precipitation from the four different forcing datasets applied in the one-year experimental LIS integration (NLDAS2, Stage IV, NMQ, and GOES QPE along columns) during four different months of October 2011, January 2012, April 2012, and July 2012 (along rows).

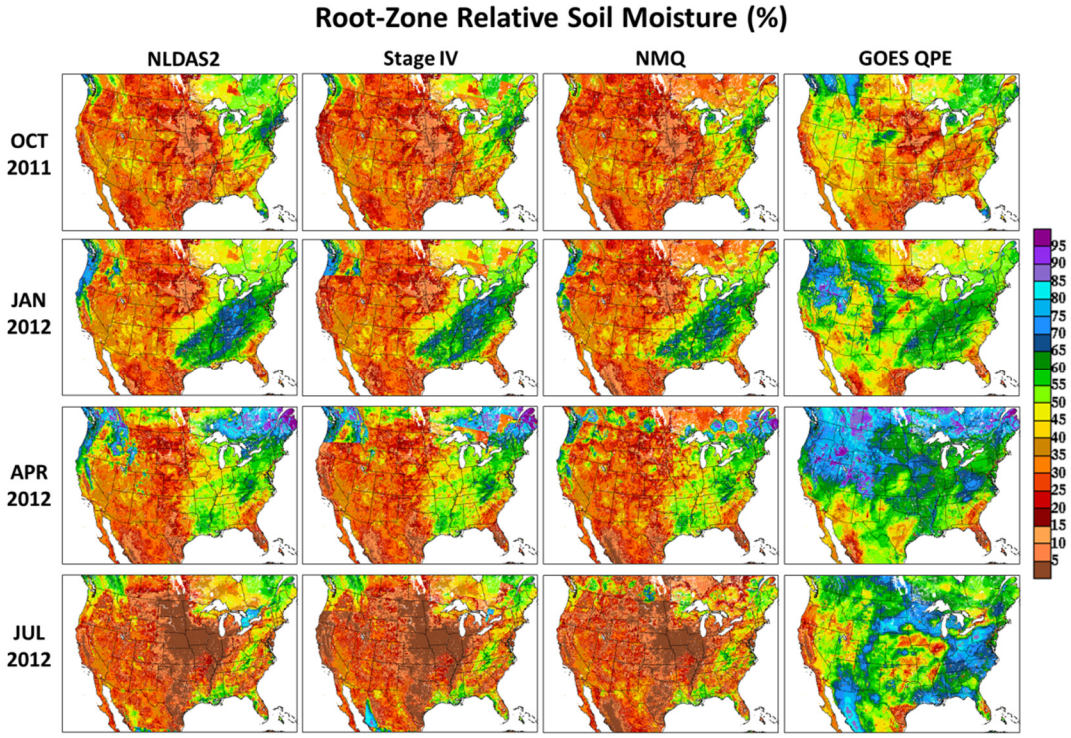

Figure 4. Depiction of the 40-100 cm relative soil moisture (ratio between wilting and saturation points, given in %; aka "available water") from the Noah land surface model within the one-year experimental LIS integrations, using the four different forcing datasets (NLDAS2, Stage IV, NMQ, and GOES QPE along columns). The valid times for the soil moisture are 0000 UTC on 31 October 2011, 29 January 2012, 28 April 2012, and 27 July 2012 in the rows indicated by the month and year, respectively.

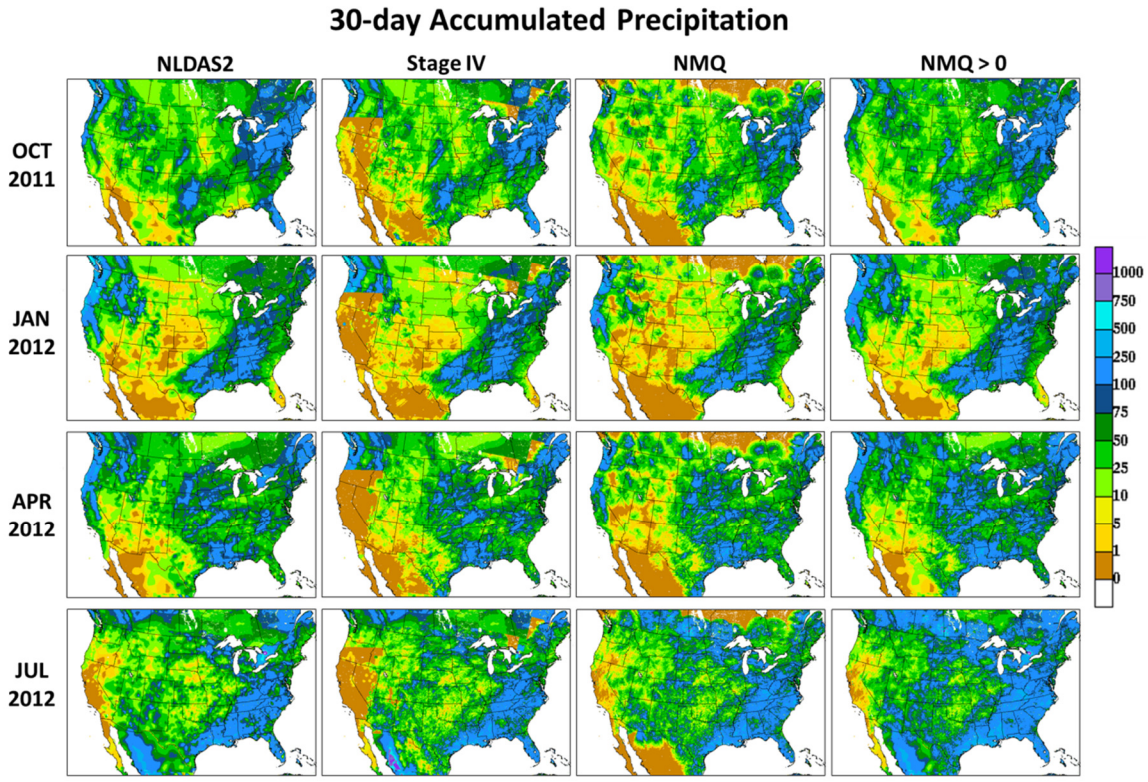

Figure 5. Same as in Figure 3, except depicting the "NMQ > 0" experiment in place of GOES QPE in the fourth column.

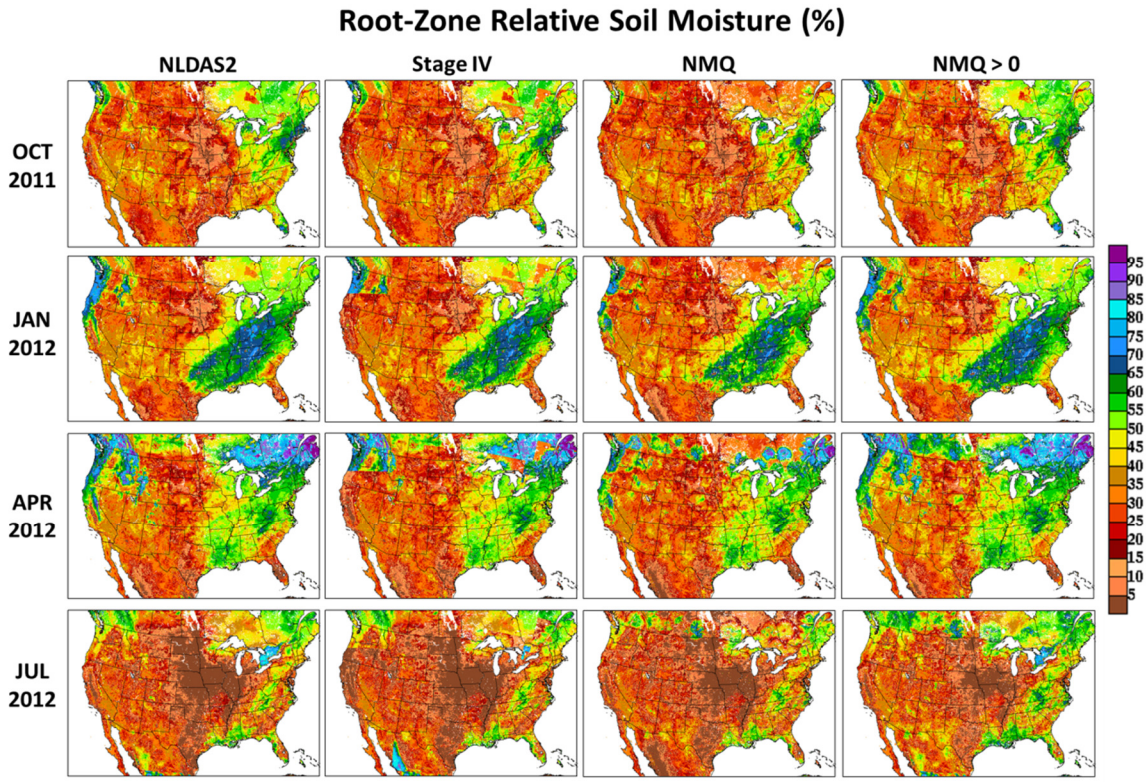

Figure 6. Same as in Figure 4, except depicting the "NMQ > 0" experiment in place of GOES QPE in the fourth column.

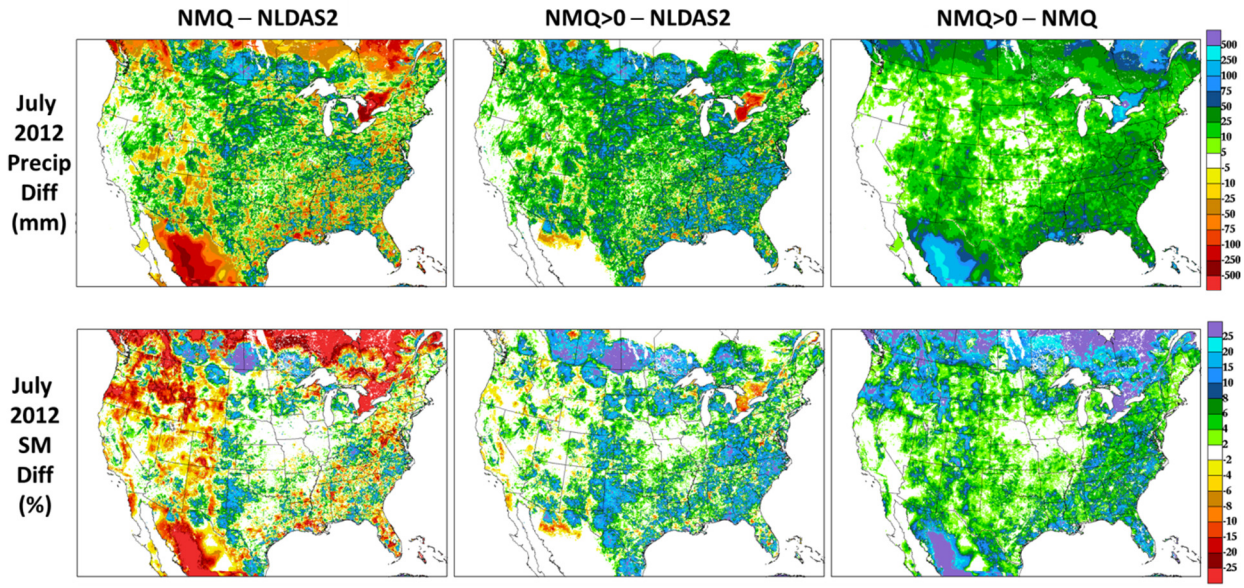

Figure 7. Differences in 30-day accumulated precipitation during July 2012 (top row) and differences in simulated 40–100 cm relative soil moisture on 0000 UTC 27 July 2012 (bottom row). Difference fields shown are for NMQ – NLDAS2 precipitation/simulations (left column), NMQ > 0 – NLDAS2 precipitation/simulations (middle column), and NMQ > 0 – NMQ precipitation/simulations (right column).